A Novel Strategy of Maximum Power Point Tracking for Photovoltaic Panels Based on Fuzzy Logic Algorithm

Mohammad EYDI, Seyyed Iman HOSSEINI SABZEVARI, Reza GHAZI

Department of Electrical Engineering, Faculty of Engineering, Ferdowsi University of Mashhad, Azadi Street, 9177948974 Mashhad, Iran

m.eydi@mail.um.ac.ir, imanhosseini@mail.um.ac.ir, rghazi@um.ac.ir

DOI: 10.15598/aeee.v18i1.3511

Abstract. *From the perspective of renewable energy industry investment, absorbing maximum power from renewable sources is a vital factor. Hence, an algorithm is required to change the operating point of renewable energy sources in different environment conditions accordingly. This paper proposes a novel algorithm for tracking the Maximum Power Point (MPP) of a Photovoltaic (PV) panel. In this paper, an auxiliary parameter based on the voltage and power of the PV panel is suggested. By adopting this parameter, independence of irradiation and temperature, the interval between the operating point and the MPP can be estimated. Furthermore, the range of the MPP voltage variations is calculated with respect to various irradiations and temperatures. Then, a novel fuzzy logic Maximum Power Point Tracking (MPPT) algorithm is proposed based on the introduced parameter and voltage variations interval of the MPP. The proposed algorithm has appropriate respond to environment condition changes with proper speed and accuracy. In addition, unlike Hill Climbing (HC) and Perturb and Observe (P&O), the proposed method has no chattering in steady state. The abovementioned claims are successfully validated via the software MATLAB/Simulink.*

Keywords

Fuzzy Logic Algorithm, MPPT, PV Panel, Range of MPPs Variations.

1. Introduction

Recently, the energy demand is enlarging enormously due to the growth of industry and increase of world population. Moreover, the shortage of fossil fuels resources and environmental problems makes Renewable Energy Sources (RES) prevalent [1], [2], and [3]. The wind and solar gained more attention because of their superior features such as low maintenance cost, the capability of employing at outland areas, wide output power range, and no fuel requirement. Although the operation cost of RESs is low, they have a high initial investment. Therefore, to improve their return on investment, maximum accessible power extraction is an important factor of the operation [3], [4], and [5]. The generated power is maximized in a specific operating point, called Maximum Power Point (MPP). As the MPP varies due to the changes in environmental conditions such as solar irradiation and temperature, a control algorithm is required to detect the MPP continuously and set the operating point accordingly [6] and [7].

Several different approaches are presented for tracking the MPP which have different accuracy, level of simplicity, range of effectiveness, convergence speed, number and type of sensors, total cost, dependency to PV panel parameters and steady state chatering [8]. Some literarure proposed sensor based methods. In these methods, the voltage of MPP and hence the duty cycle are determined by the means of measured irradiance and temperature and the PV cell characteristic. High cost because of sensor implementation, low reliability and the fact that accurate value of the panel parameters are required for operation are some of the most important disadvantages of sensor based methods [9] and [10].

According to the voltage and current relationship in a PV panel, maximum power point can be achived based on the PV voltage and current. Therefore, an MPPT algorithm can be implemented imdependent of irradiance and temperature sensors.

Different MPP tracking algorithms have been presented in the literature based on PV voltage and current. Hill Climbing (HC) [11] and [12], Perturb and Observe (P&O) [13] and [14] and Incremental Conductance (IC) [15] are some of the well-known methods. Although these methods have been used commercially, they suffer from several disadvantages. For instance, they cannot obtain high speed and accuracy at the same time. The chattering phenomenon at the steady state is another drawback of them.

In order to overcome these drawbacks, various methods had been presented. Some references utilize adaptive control strategies [14]. For instance, in [16], the voltage of MPP determined via P&O algorithm and tracked by variable voltage step size. In the proposed method, a PSO algorithm sets the voltage step size regarding to specification of the panel. The disadvantages of this method are, for example, its complexity or the necessity of a primary test to determine panel parameters.

In [17], an MPPT method based on optimization algorithm was introduced. In [18] and [19], the heuristic algorithm, in [20] the artificial bee colony, and in [21], the searching method was used. Implementation complexity, the requirement of a large number of sample points and low speed are some important drawbacks of these methods. In addition, some methods, such as [19] and [22], suffer from divergence and initial values dependency.

In [23], the panel power is first calculated in several different operation points. Then, the MPP is determined by the means of a Bat algorithm and output power of sampled points. Power fluctuation during MPP determination process and low convergence speed are some of the most important drawbacks of this method.

In some literature, hybrid methods are investigated. In [24], a hybrid approach based on P&O algorithm and fuzzy control was presented. Although the proposed algorithm improves convergence speed and eliminates parameter dependency, this method requires accurate sensors which increases the costs of the system. As the response of the PSO based methods has unconvenient dynamic characteristic, [25] suggested to combined these methods with HC algorithm. The presented results indicate that although the primarly fluctuations have improved, the dynamic response of the system contain ripple and has low speed.

In [26], a new MPPT algorithm was proposed based on Grey Wolf Optimization (GWO) and P&O. Reference [27] used the integrated Particle Swarm Optimization (PSO) and Proportional-Integral (PI) controller. The combination of P&O with Simulating Annealing (SA) and PSO are presented in [28] and [29], respectively.

In [30], a neuro-fuzzy based method was presented to decline chattering phenomena at MPP. Complexity, reduction of convergence speed at low irridations, and requirement of panel parameters are the most important disadvantages of the presented method. In [31], the authors tracked the MPP by adopting $\frac{dP}{dV}$ and SM controller. The results show that the proposed method has proper speed and accuracy. Complexity and dependency of convergence speed to irradiation and temperature are its most important drawbacks. In [32], a hybrid method based on IC and fuzzy controller had been presented which has low speed at low irradiations and high temperature, unconvenient dynamic response at the environmental condition changes, chattering, and low accuracy.

As can be seen by merging MPPT metods together, some of the aforementioned disadvantages are eliminated but their control algorithm becomes more complex. In addition, another problems arise.

In this paper, a novel method for tracking the MPP is proposed. At first, the voltage variations interval of the MPP is determined by using the one-diode model of a PV cell. In accordance with the PV cell characteristic, an auxiliary parameter is introduced which estimates the distance between operating and maximum power point, independent of irradiation and temperature. Next, by means of the Fuzzy Logic Algorithm (FLA), an MPPT algorithm based on this parameter and range of voltage variations of the MPP is implemented. Based on the simulation results, the proposed algorithm has high speed and proper accuracy performance.

This paper is organized as follows: in Sec. 2. , the PV panel model and its characteristic are presented. Furthermore, the auxiliary parameter is introduced in this section. Section 3. presents the implementation of the proposed MPPT algorithm based on the FLA, PV panel voltage, and auxiliary parameter. In addition, the interval of the voltage variations of the MPP is expressed in this section. Section 4. illustrates the simulation results of the proposed method in MATLAB/Simulink software. Finally, Sec. 5. concludes the paper.

2. System Model

The structure of a grid-connected PV panel is shown in Fig. 1. It consists of a PV panel, a voltage boost converter, and an inverter. The extracted power by the PV panel is transferred to the DC bus by means of a DC-DC converter. The inverter injects this power to the grid through the filter. The inverter power is decided by the DC bus voltage controller. In this structure, various DC-DC converter topologies with differ-

ent voltage gain can play the voltage boost converter role. For this application, the converter should have high voltage gain and continuous input current [33]. Table 1 summarizes some of the voltage boost converters and their voltage gain presented in the literature [34].

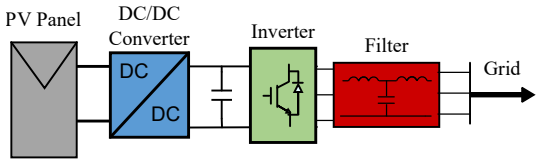

Fig. 1: The structure of a grid-connected PV panel.

Tab. 1: Suggested converter for PV applications.

Converter	Structure	Gain
boost	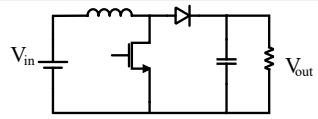	$\frac{1}{1-D}$
buck-boost	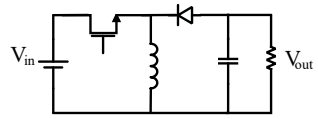	$\frac{-D}{1-D}$
cuk	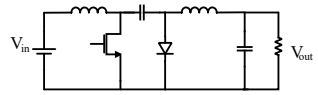	$\frac{-D}{1-D}$
sepic	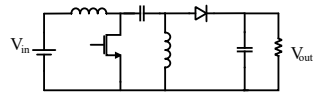	$\frac{D}{1-D}$
zeta	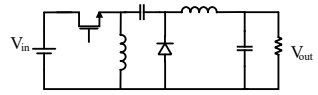	$\frac{D}{1-D}$

The most common converter, which has been used for this application, is the conventional boost converter. Since there is an inductor on the input of this converter, its input current is continuous. As the inverter controls the voltage of the capacitor, it can be assumed that the output voltage of the boost converter is constant. Hence, by setting the duty cycle of the PV panel, the input voltage can be fully controlled. In fact, the MPPT algorithm obtains the voltage of the MPP based on the irradiation and temperature. Then at this voltage, the duty cycle of the converter is determined by Eq. (1).

$$\frac{V_{out}}{V_{in}} = \frac{1}{1-D}. \tag{1}$$

Figure 2 shows the power curve of a PV panel with respect to its voltage. As shown in this figure, the amount of absorbed power in small voltages is low. As the PV voltage increases, the absorbed power increases up to the MPP. At this point, the ratio of power variation to voltage variation ($\frac{\Delta P}{\Delta V}$) is zero and with further voltage increase, the power of the PV panel will start to decrease. Rudimentary methods such as P&O and HC use this characteristic for detecting MPP.

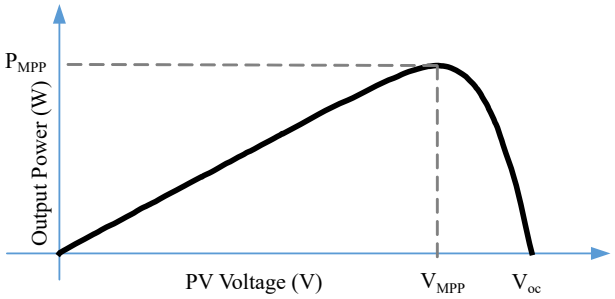

Fig. 2: Power curve of a PV cell with respect to its voltage.

An effective MPPT algorithm should have high speed and accuracy. Furthermore, it must be free from any chattering phenomenon. The high-speed operation can be achieved by increasing the Voltage Change Step Size (VCSS) but on the other hand, a large VCSS will reduce the MPPT algorithm accuracy. Therefore, in an MPPT algorithm, a trade-off should be made in order to acquire proper speed and accuracy.

An MPPT algorithm can achieve both high speed and accuracy by adjustable VCSS. When the operating point is far from the MPP, the algorithm sets a high value for VCSS to increase the speed of the operation. By approaching to the MPP, the algorithm decreases VCSS value to improve the accuracy. Therefore, an estimation of the distance between the operating point and MPP is needed to improve the operation of the system and calculate the VCSS.

Since the value of $\frac{dP}{dV}$ for the operating points, which are far from MPP, is high and low in its nearby, it seems that this parameter is suitable for MPPT step size specification.

Figure 3 shows the one-diode model of a PV cell. Based on this model, the output power of a cell can be derived from Eq. (2).

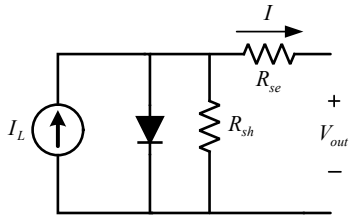

Fig. 3: One-diode model of a PV cell.

$$P = VI_L - VI_0\left(e^{A(V+R_sI)} - 1\right), \tag{2}$$

where I_L is related to the irradiation. A and I_0 are determined by Eq. (3) and Eq. (4):

$$A = \frac{q}{mkT\eta}, \tag{3}$$

$$I_0 = \frac{I_{sc}}{\frac{qV_{oc}}{e^{mkT\eta} - 1}}, \tag{4}$$

where q, m and K are elementary charge ($1.602 \cdot 10^{-19}$ C), number of series cells and Boltzmann constant, respectively. Reverse saturation current, short circuit current, and open circuit voltage are denoted as I_0, I_{sc} and V_{oc}. The $\frac{dP}{dV}$ can be obtained as follows:

$$\begin{aligned}\frac{dP}{dV} &= I_L - I_0\left(e^{A(V+R_sI)} - 1\right) + \\ &-VI_0e^{A(V+R_sI)}\left(A + AR_s\frac{dI}{dV}\right).\end{aligned} \tag{5}$$

By manipulating Eq. (5), we get:

$$\begin{aligned}&\frac{dP}{dV}\left(1 + AR_sI_0e^{A(V+R_sI)}\right) = \\ &= I\left(1 + AR_sI_0e^{A(V+R_sI)}\right) - AVI_0e^{A(V+R_sI)}.\end{aligned} \tag{6}$$

As can be seen in Eq. (6), the $\frac{dP}{dV}$ affiliates to the output power. Therefore, Eq. (6) is divided into the output power.

$$\frac{dP}{PdV} = \frac{1}{V} - \frac{\frac{AI_0}{I}e^{A(V+R_sI)}}{1 + AR_SI_0e^{A(V+R_sI)}}. \tag{7}$$

According to Eq. (7) at low voltages, $\frac{dP}{PdV}$ can be approximated by $\frac{1}{V}$ independent of irradiation and temperature.

In Tab. 2, the characteristic of a PV cell is given. Figure 4 shows the PV power, $\frac{dp}{dv}$ and $\frac{dp}{pdv}$ curves at two different irradiation, i.e. 500 and 1000 W·m^{-2}. Assume that the MPPT algorithm determined the VCSS based on $\frac{dp}{dv}$. Therefore, if the amount of the $\frac{dp}{dv}$ be high, the voltage changes will be high too. When the irradiation is equal to 1000 W·m^{-2}, operating point which their $\frac{dp}{dv}$ value is lower than 5.5 A (point a) will be considered near the MPP. Therefore, when the irradiation is low and the system operates at the A point, a low value for VCSS will be selected which decreases the operation speed. However, if the $\frac{dp}{dv}$ thereshold selected 2.7 (point b), at the irradiation of 500 W·m^{-2}, the point B (which is near MPP) will be identified as a far operating point and a high value for VCSS will be selected by the algorithm. Consequently, the algorithm may fails to identify MPP correctly.

Tab. 2: Investigated PV cell characteristic.

Parameters	Values
q (C)	$1.602 \cdot 10^{-19}$
V_{oc} (V)	46
m (-)	72
k (m^2·kg·s^{-2}·K^{-1})	$1.38 \cdot 10^{-23}$
η (-)	1.35
I_{sc} (A)	5.78

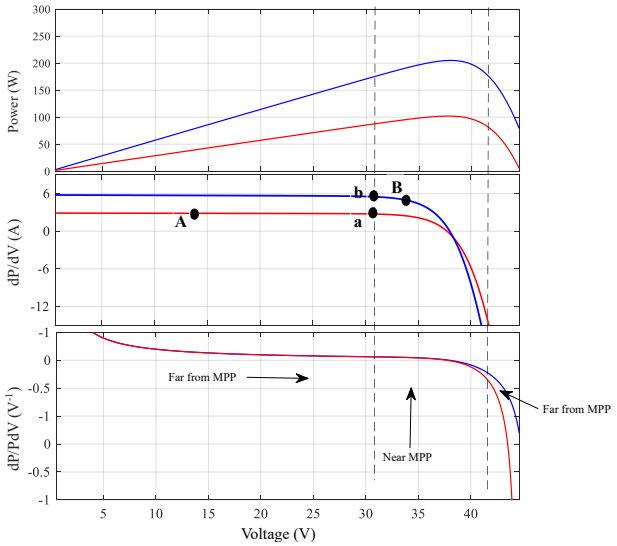

Fig. 4: The $\frac{dP}{PdV}$ and power curves for investigated PV cell.

At lower voltages than the MPP, $\frac{dP}{PdV}$ curves of two different irradiations are identical. By approaching to the MPP, the value of $\frac{dP}{PdV}$ reaches to zero and at higher voltages $\frac{dP}{PdV}$ becomes a large negative value. Therefore, the $\frac{dP}{PdV}$ is a convenient parameter for specifying MPPT step size independent of irradiation and temperature.

3. Proposed Fuzzy Logic Algorithm

As explained in the previous section, when the operating point is far from the MPP, the value of the $\frac{dP}{PdV}$ is positive. By approaching to the MPP, the value of $\frac{dP}{PdV}$ is decreased to zero. Hence, if VCSS is defined based on $\frac{dP}{PdV}$, the step size will change according to the difference of operating point from the MPP. In this paper, the FLA is adopted for the implementation of MPPT. By the help of the FLA, the MPP can be recognized with proper speed and without having an accurate model of the system, temperature sensor, and irradiation information.

3.1. Fuzzification

As the input signal of the proposed algorithm is $\frac{dP}{PdV}$, fuzzification is performed with respect to this parameter. The membership function of this parameter is shown in Fig. 5. When the operating point is at the left side of the MPP, the value of $\frac{dP}{PdV}$ is positive and its fuzzy value is equal to P. By getting closer to the MPP, the value of $\frac{dP}{PdV}$ approaches to zero and its fuzzy value would be equal to Z. At higher voltages, the value of $\frac{dP}{PdV}$ is negative and its fuzzy value will change from Z to N.

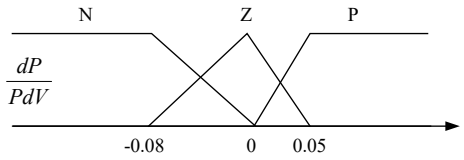

Fig. 5: The membership function of the input.

When the system operates at the MPP and the irradiation changes, the value of $\frac{dP}{PdV}$ will be high. In this case, the MPPT algorithm assumes that the operating point is far from the MPP and sets a high value for VCSS. This leads to undesirable behavior of the MPPT algorithm.

In order to improve the system response, additional paramerter is required to help the control algorithm tracks the MPP correctly when the enviroment conditions changes and prevent the selection of high value for VCSS.

By equalling Eq. (7) to zero we obtain the maximum power points with respect to various irradiations and temperatures.

$$V = \frac{Ie^{-A(V+R_sI)}}{AI_0} + R_S I. \tag{8}$$

From Eq. (2), Eq. (8), and Tab. 2, the MPP voltage is 38 V at 1000 W·m^{-2} irradiation and temperature of 25 °C. In case of diversity of environment temperature from −10 to 50 °C and irradiation from 100 to 1000 W·m^{-2}, maximum and minimum of the MPP voltage for presented PV cell are 44 and 30 V, respectively. Hence, the MPP voltage is between 30 and 44 V consistently.

As the MPPs voltages are always in a specific area for a wide range of irradiations and temperatures, using voltage as a second parameter would be beneficial. When the voltage is in the area obtained by Eq. (8) and $\frac{dP}{PdV}$ has a high value, since the MPP is in the vicinity of the operating point, a small value should be selected for VCSS. Therefore, for a better performance of the algorithm, the PV voltage and $\frac{dP}{PdV}$ are selected as control signals. The membership function of the PV voltage is shown in Fig. 6. As shown in this figure, at low, medium, and high voltages its fuzzy value is equal to LS, MPP, and RS, respectively.

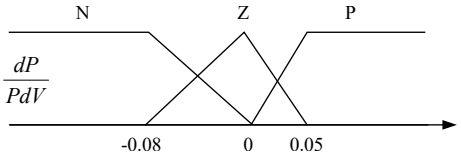

Fig. 6: The membership function of the voltage.

3.2. Fuzzy Rules

Positive, negative and zero values of $\frac{dP}{PdV}$ indicate that the PV voltage should be increased, decreased and remained unchanged, respectively. If the irradiation changes, despite variation of the output power, the voltage remains almost the same. This results in a high value of $\frac{dP}{PdV}$. In this case, as the PV voltage is in the MPP interval, the FLA sets a short negative or positive value for VCSS based on the sign of $\frac{dP}{PdV}$.

Fuzzy rules are shown in Tab. 3. For instance, if the fuzzy value of $\frac{dP}{PdV}$ is high, then the algorithm checks the PV voltage. If the PV voltage is low, the output fuzzy value will be PB. If it exists in the MPP area, the obtained output fuzzy logic would be PM. Fig. 7 shows the membership function of the output.

Tab. 3: Fuzzy rules.

Parameters		$\frac{\mathbf{dP}}{\mathbf{PdV}}$ **(V^{-1})**		
		N	**Z**	**P**
V (V)	**LS**	ZN	PM	PB
	MPP	NM	ZN	PM
	RS	NB	NM	ZN

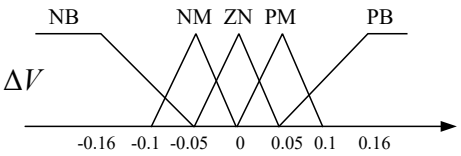

Fig. 7: The membership function of the output.

3.3. Defuzzification

The final step in FLA is determining output value (converter duty cycle in this paper) that is called defuzzification. One of the well-known defuzzification operators is the Center Of Gravity (COG). The COG is a classic method that calculates the center of the gravity of the area under the membership function. This method is simple and has a suitable speed. COG is computed by

Eq. (9).

$$\Delta V_{pv} = COG(A) = \frac{\sum_{1}^{n} xA(x)}{\sum_{1}^{n} A(x)}, \tag{9}$$

where n and $A(x)$ are the numbers of the fuzzy rules and the probability distribution of rule x. For approaches to the MPP, the computed value of Eq. (9) is added to the PV voltage.

$$V_{pv}(k) = V_{pv}(k-1) + \Delta V_{pv}. \tag{10}$$

In the following, $V_{pv}(k)$ is used as the reference voltage for DC/DC converter and its duty cycle is specified based on this value.

4. Simulation Results

The simulation results of the proposed algorithm are described in this section. The simulated system characteristics are summarized in Tab. 2 and Tab. 4.

Tab. 4: PV Panel Characteristic.

Parameters	Values
Parallel String	2
Series Module per String	3
Maximum Power (W)	206
Short circuit Current (A)	11.56
Open circuit Voltage (V)	138.9
Voltage at MPP (V)	114.5
Current at MPP (A)	10.8

Figure 8 shows the system structure. As the parasitic elements are included in the simulation, the reference voltage is not followed through the Eq. (1) and therefore, PI controller is utilized to determine duty cycle.

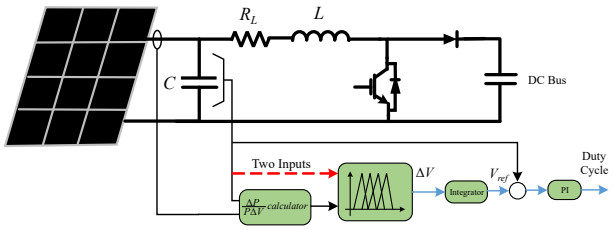

Fig. 8: The system structure.

As explained in the previous section, for improving the performance of the algorithm, it is beneficial to use PV voltage as the second control parameter in addition to the $\frac{dP}{PdV}$. Utilization of PV voltage will improve the dynamic response and has no effect on the steady state. To verify the PV voltage utilization effect, simulations are performed in two statuses, with and without PV voltage. To prove that the algorithm provides good speed and high accuracy, the system is simulated at zero voltage with step-changing irradiation and temperature.

Figure 9 and Fig. 10 show the irradiation and temperatoure variations of the simulated system. As can be seen, at first the irradiation is equal to 1000 W·m^{-2}. It decreases to 500 W·m^{-2} at $t = 10$ s and increases to 800 W·m^{-2} at $t = 15$ s. The temperature increases at $t = 20$ s to 50 °C and decreases to 35 °C at $t = 25$ s. Therfore MPP changes at these times.

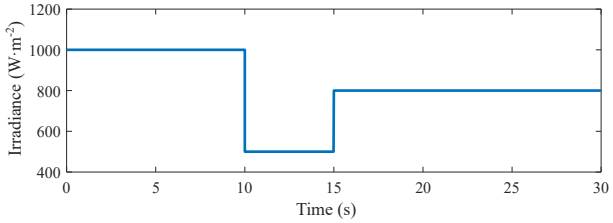

Fig. 9: The irradiation.

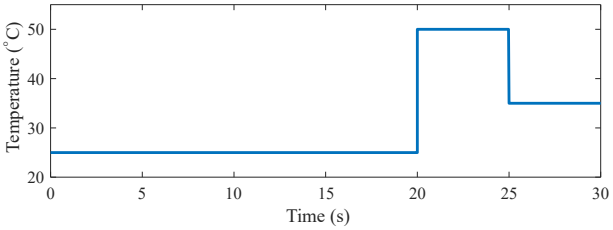

Fig. 10: The ambient temperature.

Figure 11 shows the PV voltage curve. The voltage is zero at the beginning. Therefore, the value of VCSS is selected high. By approaching toward the MPP the step size is reduced by the algorithm accordingly. Consequently, the MPPT operates with suitable speed. As at this time interval, the irradiance and temperature does not change, the PV voltage in both methode is same. After a period of time, the irradiation is reduced instantaneously. In the single input scenario, the algorithm assumes that the operating point is far from MPP, so it sets a high value for VCSS that causes overshoot at the PV voltage curve. In contrast, when the PV voltage is used as a second control parameter, the algorithm recognizes that the MPP is in the vicinity of the operating point. Hence a small step size is chosen which leads to desired dynamic response.

At $t = 20$ s, the panel temperature increases. So the power and the capacitor voltage decreases. If the ampelitutde of the power change is high, the $\frac{dp}{pdv}$ would have a high positive value. Therefore, in single-input algorithm, a high positive value will be set for VCSS. If the ampelitutde of the voltage change is high, the operating point will be moved to the right side of the MPP and at the next step the algorithm will decrease the voltage to track the MPP. However, in double-input method, both the $\frac{dp}{pdv}$ and voltage changes are inves-

Tab. 5: Extracted power.

Parameters		Irradiation (W·m^{-2}) & Temperature (°C)				
		600 & 25	**800 & 25**	**1000 & 25**	**800 & 50**	**800 & 35**
Power (W)	**Maximum Accessible Power**	613.5	988	1236	889	948.6
	Single-input Maximum Power	612	984.2	1232	887.3	946.5
	Double-input Maximum Power	611.9	984.6	1232	887.6	946.3

tigated in each step. Since at $t = 20$ s the voltage is inside the MPP area, although the $\frac{dp}{pdv}$ value is high, a small value will be selected for VCSS. As a result, the system shows better dynamic response in compare to the single-input method.

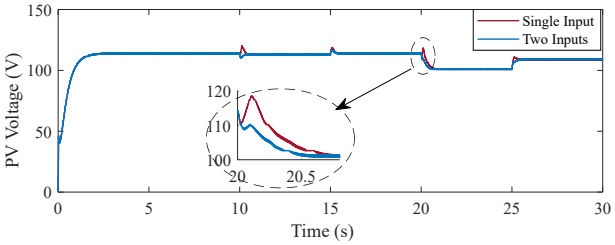

Fig. 11: The PV voltage.

The duty cycle changes are shown in Fig. 12. The duty cycle is approximately 70 regarding to output voltage (400 V) and PV voltage range. Since the voltage changes in single-input method are more than double-input method, the duty cycle changes are less in double-input method.

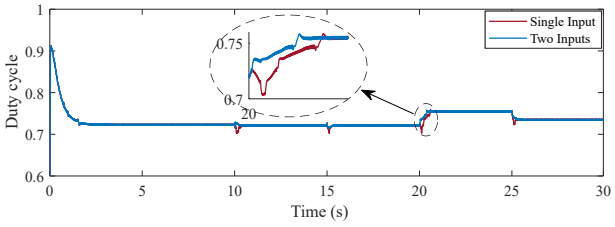

Fig. 12: Converter duty cycle.

The PV power is shown in Fig. 13. When the enviromental condition changes, the voltage deviation from MPP voltage are greater in single-input algorithm than double-input method. Therefore, as can be seen in Fig. 13, the output power experiences higher undershoot in single-input method. This problem is tackled in the double-input method by considering a second control parameter. As the PV voltage is not contributed in determinig MPP in steady state, the output power in steady state is identical for both approaches.

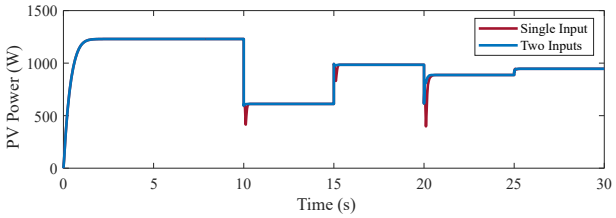

Fig. 13: PV output power.

The $\frac{dP}{PdV}$ curve is shown in Fig. 14. At the begging, the operating point is far from MPP and $\frac{dP}{PdV}$ value is high. When the operating point moves towards the MPP, this value decreases to zero.

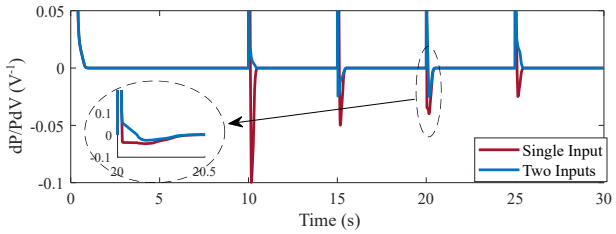

Fig. 14: The auxiliary parameter.

When the irradiation increases (decreases) or the temperature declined (rised), the PV power and capacitor voltage will increase (reduce). As the power and voltage changes have same sign, $\frac{dp}{pdv}$ obtains a positive value. Therefore, when the environmental conditions changes, the voltage of the operating point is assumed less than MPP voltage and a high positive value will be set for VCSS in single-input method. As a result in this method, the voltage will contain overshoots which results in operating at the right side of the MPP ($\frac{dp}{pdv} < 0$). However, in double-input method, as the value of the VCSS is low, the severity of the overshoots are restricted.

Therefore, when the enviromental condition changes, the voltage variation is small and the power variation is high. So the amount of the $\frac{dP}{PdV}$ is quite high. Therefore, to improve dynamic behaviour of the MPPT algorithm, adopting voltage as the second parameter is essential.

Table 5 verifies the algorithm accuracy. This table shows the maximum absorbed and accessible power. It indicates that the proposed algorithm can track the MPP with good accuracy. As it is evident, both algorithms (single input and double inputs) have the same steady-state response.

5. Conclusion

In this paper, a novel MPPT algorithm for a PV panel was proposed. At first, the system structure was analyzed and then it is shown that the voltage and therfore the transferred power from the PV panel can be efficively controlled by the boost converter. It is elaborated that with the use of $\frac{dP}{dV}$, the MPP cannot be tracked properly, as this value is associated with irradiation and temperature. Thus, another parameter is introduced. The proposed parameter estimates the relative difference of the operating point with respect to the MPP, independent of irradiation and temperature. In addition to that, the voltage changes interval of MPP of a PV panel with respect to various irradiation and temperature are calculated. Then an MPPT algorithm based on FLA and the proposed parameter is implemented. It is shown that the single input algorithm provides an improper dynamic response, so the voltage of the PV panel is taken as a second control parameter. Simulation results indicate that the proposed algorithm with two control parameters presents suitable speed and accuracy with the proper dynamic response for a wide range of irradiation and temperature changes.

References

[1] QIN, Y., F. TONG, G. YANG and D. L. MAUZERALL. Challenges of using natural gas as a carbon mitigation option in China. *Energy Policy*. 2018, vol. 117, iss. 1, pp. 457–462. ISSN 0301-4215. DOI: 10.1016/j.enpol.2018.03.004.

[2] PILLAI, D. S., J. P. RAM, M. S. S. NIHANTH and N. RAJASEKAR. A simple, sensorless and fixed reconfiguration scheme for maximum power enhancement in PV systems. *Energy Conversion and Management*. 2018, vol. 172, iss. 1, pp. 402–417. ISSN 0196-8904. DOI: 10.1016/j.enconman.2018.07.016.

[3] Renewables 2019 Global Status Report. In: *REN21* [online]. 2019. Available at: `https://www.ren21.net/wp-content/uploads/2019/05/gsr_2019_full_report_en.pdf`.

[4] DEPURU, S. R. and M. MAHANKALI. Performance Analysis of a Maximum Power Point Tracking Technique using Silver Mean Method. *Advances in Electrical and Electronic Engineering*. 2018, vol. 16, iss. 1, pp. 25–35. ISSN 1804-3119. DOI: 10.15598/aeee.v16i1.2249.

[5] FARIAS-ROCHA, A. P., K. M. K. HASSAN, J. R. R. MALIMATA, G. A. SANCHEZ-CUBEDO and L. R. ROJAS-SOLORZANO. Solar photovoltaic policy review and economic analysis for on-grid residential installations in the Philippines. *Journal of Cleaner Production*. 2019, vol. 223, iss. 1, pp. 45–56. ISSN 0959-6526. DOI: 10.1016/j.jclepro.2019.03.085.

[6] DADKHAH, J. and M. NIROOMAND. Real-Time MPPT Optimization of PV Systems by Means of DCD-RLS Based Identification. *IEEE Transactions on Sustainable Energy*. 2018, vol. 10, iss. 4, pp. 2114–2122. ISSN 1949-3037. DOI: 10.1109/TSTE.2018.2878826.

[7] NAICK, B. K., K. CHATTERJEE and T. K.CHATTERJEE. Assessment of MPPT Techniques During the Faulty Conditions of PV System. *Advances in Electrical and Electronic Engineering*. 2018, vol. 16, iss. 1, pp. 15–24. ISSN 1804-3119. DOI: 10.15598/aeee.v16i1.2581.

[8] BELHACHAT, F. and C. LARBES. A review of global maximum power point tracking techniques of photovoltaic system under partial shading conditions. *Renewable and Sustainable Energy Reviews*. 2018, vol. 92, iss. 1, pp. 513–553. ISSN 1364-0321. DOI: 10.1016/j.rser.2018.04.094.

[9] LI, L.-L., G.-Q. LIN, M.-L. TSENG, K. TAN and M. K. LIM. A maximum power point tracking method for PV system with improved gravitational search algorithm. *Applied Soft Computing*. 2018, vol. 65, iss. 1, pp. 333–348. ISSN 1568-4946. DOI: 10.1016/j.asoc.2018.01.030.

[10] YILMAZ, U., O. TURKSOY and A. TEKE. Improved MPPT method to increase accuracy and speed in photovoltaic systems under variable atmospheric conditions. *International Journal of Electrical Power & Energy Systems*, vol. 113, iss. 1, pp. 634–651. ISSN 0142-0615. DOI: 10.1016/j.ijepes.2019.05.074.

[11] LIU, H.-D., C.-H. LIN, K.-J. PAI and Y.-L. LIN. A novel photovoltaic system control strategies for improving hill climbing algorithm efficiencies in consideration of radian and load effect. *Energy Conversion and Management*. 2018, vol. 165, iss. 1, pp. 815–826. ISSN 0196-8904. DOI: 10.1016/j.enconman.2018.03.081.

[12] YOROZU, T., M. HIRANO, K. OKA and Y. TAGAWA. Electron Spectroscopy Studies on Magneto-Optical Media and Plastic Substrate Interface. *IEEE Translation Journal on Magnetics in Japan*, vol. 2, iss. 8, pp. 740–741. ISSN 2375-0545. DOI: 10.1109/TJMJ.1987.4549593.

[13] SHER, H. A., A. F. MURTAZA, A. NOMAN, K. E. ADDOWEESH, K. AL-HADDAD and M. CHIABERGE. A New Sensorless Hybrid MPPT Algorithm Based on Fractional Short-Circuit Current Measurement and P&O MPPT. *IEEE Transactions on Sustainable Energy*. 2015, vol. 6, iss. 4, pp. 1426–1434. ISSN 1949-3037. DOI: 10.1109/TSTE.2015.2438781.

[14] ALIK, R. and A. JUSOH. An enhanced P&O checking algorithm MPPT for high tracking efficiency of partially shaded PV module. *Solar Energy*. 2018, vol. 163, iss. 1, pp. 570–580. ISSN 0038-092X. DOI: 10.1016/j.solener.2017.12.050.

[15] KUMAR, N., I. HUSSAIN, B. SINGH and B. K. PANIGRAHI. Self-Adaptive Incremental Conductance Algorithm for Swift and Ripple-Free Maximum Power Harvesting From PV Array. *IEEE Transactions on Industrial Informatics*. 2017, vol. 14, iss. 5, pp. 2031–2041. ISSN 1941-0050. DOI: 10.1109/TII.2017.2765083.

[16] HARRAG, A. and S. MESSALTI. PSO-based SMC variable step size P&O MPPT controller for PV systems under fast changing atmospheric conditions. *International Journal of Numerical Modelling: Electronic Networks, Devices and Fields*. 2019, vol. 32, iss. 5, pp. 1–24. ISSN 0894-3370. DOI: 10.1002/jnm.2603.

[17] SUNDARESWARAN, K., S. PEDDAPATI and S. PALANI. MPPT of PV Systems Under Partial Shaded Conditions Through a Colony of Flashing Fireflies. *IEEE Transactions on Energy Conversion*. 2014, vol. 29, iss. 2, pp. 463–472. ISSN 1558-0059. DOI: 10.1109/TEC.2014.2298237.

[18] LIAN, K. L., J. H. JHANG and I. S. TIAN. A Maximum Power Point Tracking Method Based on Perturb-and-Observe Combined With Particle Swarm Optimization. *IEEE Journal of Photovoltaics*. 2014, vol. 4, iss. 2, pp. 626–633. ISSN 2156-3403. DOI: 10.1109/JPHOTOV.2013.2297513.

[19] ISHAQUE, K. and Z. SALAM. A Deterministic Particle Swarm Optimization Maximum Power Point Tracker for Photovoltaic System Under Partial Shading Condition. *IEEE Transactions on Industrial Electronics*. 2012, vol. 60, iss. 8, pp. 3195–3206. ISSN 1557-9948. DOI: 10.1109/TIE.2012.2200223.

[20] BENYOUCEF, A. S., A. CHOUDER, K. KARA and S. SILVESTRE. Artificial bee colony based algorithm for maximum power point tracking (MPPT) for PV systems operating under partial shaded conditions. *Applied Soft Computing*. 2015, vol. 32, iss. 1, pp. 38–48. ISSN 1568-4946. DOI: 10.1016/j.asoc.2015.03.047.

[21] ZHOU, L., Y. CHEN, K. GUO and F. JIA. New Approach for MPPT Control of Photovoltaic System With Mutative-Scale Dual-Carrier Chaotic Search. *IEEE Transactions on Power Electronics*. 2010, vol. 26, iss. 4, pp. 1038–1048. ISSN 1941-0107. DOI: 10.1109/TPEL.2010.2078519.

[22] MOHAPATRA, A., B. NAYAK, P. DAS and K. B. MOHANTY. A review on MPPT techniques of PV system under partial shading condition. *Renewable and Sustainable Energy Reviews*. 2017, vol. 80, iss. 1, pp. 854–867. ISSN 1364-0321. DOI: 10.1016/j.rser.2017.05.083.

[23] TEY, K. S., S. MEKHILEF and M. SEYEDMAHMOUDIAN. Implementation of BAT Algorithm as Maximum Power Point Tracking Technique for Photovoltaic System Under Partial Shading Conditions. In: *2018 IEEE Energy Conversion Congress and Exposition (ECCE)*. Portland: IEEE, 2018, pp. 2531–2535. ISBN 978-1-4799-7312-5. DOI: 10.1109/ECCE.2018.8557460.

[24] BAHRAMI, M., R. GAVAGSAZ-GHOACHANI, M. ZANDI, M. PHATTANASAK, G. MARANZANAA, B. NAHID-MOBARAKEH, S. PIERFEDERICIA and F. MEIBODY-TABAR. Hybrid maximum power point tracking algorithm with improved dynamic performance. *Renewable Energy*. 2019, vol. 130, iss. 1, pp. 982–991. ISSN 0960-1481. DOI: 10.1016/j.renene.2018.07.020.

[25] CHAIEB, H. and A. SAKLY. A novel MPPT method for photovoltaic application under partial shaded conditions. *Solar Energy*. 2018, vol. 159, pp. 291–299. ISSN 0038-092X. DOI: 10.1016/j.solener.2017.11.001.

[26] MOHANTY, S., B. SUBUDHI and P. K. RAY. A Grey Wolf-Assisted Perturb & Observe MPPT Algorithm for a PV System. *IEEE Transactions on Energy Conversion*. 2016, vol. 32, iss. 1, pp. 340–347. ISSN 1558-0059. DOI: 10.1109/TEC.2016.2633722.

[27] KERMADI, M. and E. M. BERKOUK. A Hybrid PSO-PI Based Maximum Power Point Tracking Algorithm using Adaptive Sampling Time Strategy. In: *2015 4th International Conference on Electrical Engineering (ICEE)*. Boumerdes:

IEEE, 2015, pp. 1–6. ISBN 978-1-4673-6673-1. DOI: 10.1109/INTEE.2015.7416787.

[28] LYDEN, S. and M. E. HAQUE. A Hybrid Simulated Annealing and Perturb and Observe Method for Maximum Power Point Tracking in PV Systems Under Partial Shading Conditions. In: *2015 Australasian Universities Power Engineering Conference (AUPEC)*. Wollongong: IEEE, 2015, pp. 1–6. ISBN 978-1-4799-8725-2. DOI: 10.1109/AUPEC.2015.7324803.

[29] YANG, Z., Q. DUAN, J. ZHONG, M. MAO and Z. XUN. Analysis of Improved PSO and Perturb & Observe Global MPPT Algorithm for PV Array Under Partial Shading Condition. In: *2017 29th Chinese Control And Decision Conference (CCDC)*. Chongqing: IEEE, 2017, pp. 549–553. ISSN 1948-9447. DOI: 10.1109/CCDC.2017.7978154.

[30] HARRAG, A. and S. MESSALTI. IC-based Variable Step Size Neuro-Fuzzy MPPT Improving PV System Performances. *Energy Procedia*. 2019, vol. 157, pp. 362–374. ISSN 1876-6102. DOI: 10.1016/j.egypro.2018.11.201.

[31] VALENCIAGA, F. and F. A. INTHAMOUSSOU. A novel PV-MPPT method based on a second order sliding mode gradient observer. *Energy Conversion and Management*. 2018, vol. 176, pp. 422–430. ISSN 0196-8904. DOI: 10.1016/j.enconman.2018.09.018.

[32] YILMAZ, U., A. KIRCAY and S. BOREKCI. PV system fuzzy logic MPPT method and PI control as a charge controller. *Renewable and Sustainable Energy Reviews*. 2018, vol. 81, pp. 994–1001. ISSN 1364-0321. DOI: 10.1016/j.rser.2017.08.048.

[33] BANAEI, M. R. and S. G. SANI. Analysis and Implementation of a New SEPIC-Based Single-Switch Buck–Boost DC–DC Converter With Continuous Input Current. *IEEE Transactions on Power Electronics*. 2018, vol. 33, iss. 12, pp. 10317–10325. ISSN 1941-0107. DOI: 10.1109/TPEL.2018.2799876.

[34] FOROUZESH, M., Y. P. SIWAKOTI, S. A. GORJI, F. BLAABJERG and B. LEHMAN. Step-Up DC–DC Converters: A Comprehensive Review of Voltage-Boosting Techniques, Topologies, and Applications. *IEEE Transactions on Power Electronics*. 2017, vol. 32, iss. 12, pp. 9143–9178. ISSN 1941-0107. DOI: 10.1109/TPEL.2017.2652318.

About Authors

Mohammad EYDI was born in Mashhad, Iran in 1991. He received the B.Sc. degree in Power Engineering from Shahrood University of Technology and the M.Sc. degree in Power Electronics from the Tehran University, Iran in 2013 and 2015, respectively. He is currently study toward Ph.D. at the Ferdowsi University of Mashhad. His research interests are microgrids, power electronics converters and renewable energy systems.

Seyyed Iman HOSSEINI SABZEVARI was born in Mashhad, Iran in 1990. He received the B.Sc. degree in Power Engineering and M.Sc. degree in Power Electronics from Ferdowsi University of Mashhad in 2013 and 2019, respectively. His main research interests are electric vehicles, energy sources, power electronics converters, electric drives and renewable energy systems.

Reza GHAZI was born in Semnan, Iran in 1952. He received his B.Sc., degree (with honors) from Tehran University of Science and Technology, Tehran, Iran in 1976. In 1986 he received his M.Sc. degree from Manchester University, Institute of Science and Technology (UMIST) and the Ph.D. degree in 1989 from University of Salford UK, all in electrical engineering. Following receipt of the Ph.D. degree, he joined the faculty of engineering Ferdowsi University of Mashhad, Iran as an Assistant Professor of electrical engineering. He is now Professor of Electrical Engineering in Ferdowsi University of Mashhad, Iran. His main research interests are reactive power control, FACTS devices, application of power electronic in power systems, renewable energy sources, distributed generation, restructured power systems control and analysis. He has published over 100 papers in these fields including three books.